Theory of the soliton self-frequency shift compensation by the resonant radiation in photonic crystal fibers

F. Biancalana, D. V. Skryabin,* and A. V. Yulin
Department of Physics, University of Bath, Bath BA2 7AY, United Kingdom
(Received 5 January 2004; published 30 July 2004)

We develop a theory of the soliton self-frequency shift compensation by the resonant radiation recently observed in photonic crystal fibers. Our approach is based on the calculation of the soliton plus radiation solution of the generalized nonlinear Schrödinger (GNLS) equation and on subsequent use of the adiabatic theory leading to a system of equations governing evolution of the soliton parameters in the presence of the Raman effect and radiation. Our theoretical results are found to be in good agreement with direct numerical modeling of the GNLS equation.

DOI: 10.1103/PhysRevE.70.016615 PACS number(s): 42.81.Dp, 42.65.Tg, 42.70.Qs

I. INTRODUCTION

The recent advent of photonic crystal fibers (PCFs) opens many interesting opportunities for fundamental and applied research in different branches of nonlinear optics. The prime reason for this is that PCFs offer numerous ways to control their nonlinear and dispersive characteristics, for reviews see Refs. [1–5]. For example, in silica core PCFs nonlinearity can be enhanced by the small modal area and group velocity dispersion (GVD) can be controlled by the engineering of the photonic crystal cladding [6,7]. The hollow-core band-gap guiding PCFs can be filled with different gases and used for a variety of nonlinear optical experiments in the low loss and diffraction free geometries with very long interaction distances [8–10].

One of the widely used applications of solid-core PCFs is in generation of optical supercontinuum [11–14]. Full theoretical understanding of this process is still lacking and its possible connections with turbulence theories in Hamiltonian models [15] are waiting to be established. Another interesting and nontrivial nonlinear effect which has been recently observed in PCFs with ultrasmall silica cores is the cancellation of the Raman self-frequency shift of the solitons accompanied by the exponential amplification of the resonant radiation [7]. The resonant radiation emitted by the fiber solitons in the presence of the higher order dispersions has been known for more than a decade, see, e.g., [16–22] and it has been recently shown to play a role in the formation of the blue wing of the supercontinuum spectra generated in PCFs [12].

Telecom fibers have reasonably flat GVD profiles in the practically relevant frequency range, and small *positive* GVD slopes in these fibers do not lead to substantial radiation. Therefore, the resonant radiation effect on solitons in telecom fibers has been considered so far as merely one of many loss mechanisms. The distinct feature of the PCF used in Ref. [7] is that it has two zero GVD points and the frequency interval of the anomalous GVD has a very steep *negative* GVD slope. This interval is located on the red side of the spectral window with anomalous GVD. Therefore, the Raman effect [23,24] unavoidably pulls the femtosecond solitons into the region of the negative GVD slope, where striking and unattainable in standard telecom fibers dynamics takes place [7]. Under these conditions the solitons generate the exponentially growing redshifted radiation band. The redshifted radiation exerts pressure on the soliton itself and the soliton self-frequency shift gets compensated almost exactly [7]. The primary objective of this work is to develop a comprehensive theory of the effects reported in Ref. [7]. Radiation pressure on the soliton leading to the drift of the mean soliton frequency and group velocity, also known as the spectral recoil effect, has been previously reported in [19–22]. However, analysis of the combined action of the recoil and Raman effects appears to be missing in the known to us literature. Pulling of the soliton frequency by the Raman effect towards the zero GVD point has been previously suggested as the mechanism for the adiabatic soliton compression [25]. However, Ref. [25] and subsequent theoretical work [18] do not account for the spectral recoil and do not report the soliton self-frequency shift compensation effect observed in [7] and theoretically analyzed below.

We organize this paper in the following way. First, we introduce the model equation and derive resonance conditions for fibers with frequency dependent GVD. After this we calculate analytically the amplitude of the emitted radiation using an approach generalizing and improving the previously known. Then, knowing dependence of the radiation amplitude and frequency on the soliton parameters, we develop an adiabatic theory of the soliton evolution, explaining the self-frequency shift compensation observed in Ref. [7]. Finally, we conclude by putting our results into the context of the various soliton theories and of recent and past experimental efforts.

II. MODEL EQUATION

We assume that dynamics of the dimensionless amplitude $A(t,z)$ of the fundamental fiber mode is governed by the generalized NLS equation

*Author to whom correspondence should be addressed.
URL: http://staff.bath.ac.uk/pysdvs
Electronic address: d.v.skryabin@bath.ac.uk

$$\partial_z A = iD(i\partial_t)A + iA\int_{-\infty}^{+\infty} R(t')|A(t-t',z)|^2 dt'. \qquad (1)$$

To avoid any ambiguity in the analytical expressions we adopt the convention of using round brackets $(\cdot\cdot)$ to indicate arguments of functions or operators and $[\cdot\cdot]$, $\{\cdot\cdot\}$ for all other purposes. The dispersion operator in Eq. (1) is given by

$$D(i\partial_t) \equiv \sum_{m=2}^{M} \frac{\tau^{2-m}\partial_\omega^{m-2}\beta_2(\omega_0)}{m!\,|\beta_2(\omega_0)|}[i\partial_t]^m, \qquad (2)$$

where τ is the characteristic time close to the pulse duration. $R(t)$ is the response function of the material, which is silica glass in our case:

$$R(t) = [1-\theta]\Delta(t) + \theta\frac{\tau_1^2+\tau_2^2}{\tau_1\tau_2^2}\Theta(t)e^{-t/\tau_2}\sin\frac{t}{\tau_1}. \qquad (3)$$

Here, $\Delta(t)$ and $\Theta(t)$ are, respectively, delta and Heaviside functions. Equation (3) includes the instantaneous electronic and delayed Raman contributions with $\theta=0.18$, $\tau_1=12.2fs/\tau$, and $\tau_2=32fs/\tau$ [24]. t is the time in the reference frame moving with group velocity $v_0=v(\omega_0)$ and measured in the units of τ: $t=[T-z/v_0]/\tau$, where T is the physical time. $z=Z/L_{gvd}$, where Z is the distance along the fiber and $L_{gvd}=\tau^2/|\beta_2(\omega_0)|$ is the GVD length. Field amplitude A is measured in the units of $N\sqrt{P_0}=N/\sqrt{\gamma L_{gvd}}$, where γ is the nonlinear parameter of the fiber [24]. N^2 is the ratio of the peak power of the pump pulse to the P_0, which is the peak power of a fundamental soliton with duration τ.

Let us stress here, the dispersion operator D introduced above is not necessarily a Taylor expansion near the reference frequency, but it can be considered as a numerical fit into the experimentally measured fiber GVD characteristic. Therefore, it correctly describes dispersion of a wave which is either detuned initially or drifts gradually to the spectral regions lying arbitrarily far from ω_0. If the GVD profile is given by $\beta_2(\omega)$, then it can be fitted with a polynomial function: $\beta_2(\omega)=\Sigma_{m=0}^{M} b_{2+m}[\omega-\omega_0]^m$, where ω_0 is an arbitrary reference frequency. Equations similar to Eq. (1) have been previously used in several studies of pulse propagation in fibers, see, e.g., Refs. [6,7,13,26] and references therein, and have demonstrated reliable replication of the experimental measurements in PCFs [6,7,13]. Compared with Refs. [6,7] we have neglected here the self-steepening term [24]. This is because, as our numerical modeling has demonstrated, it has no qualitative and only small quantitative effect on the results described below, see also Sec. V.

III. SOLITON DRESSED BY THE RADIATION

A. Resonance frequencies

In order to describe influence of the Raman effect on the radiating soliton we first find the radiation field and then consider soliton dressed by the radiation as the zero order approximation to the solution of Eq. (1) treating the Raman term as a perturbation, see Sec. IV.

Generalization of the single soliton solution of the ideal NLS equation gives the following expression:

$$A = F(\xi)e^{-i\delta_s t + i[D_s+q]z}, \quad \xi = t - D_s' z,$$

$$F(\xi) = \sqrt{2q}\ \mathrm{sech}\left(\frac{\xi}{w}\right), \quad w = \sqrt{\frac{-D_s''}{2q}}, \qquad (4)$$

for the approximate soliton solution of Eq. (1), where GVD varies with frequency. Physical pulse duration is given by τw. $\delta_s=[\omega_s-\omega_0]\tau$ is the detuning of the soliton frequency ω_s from the reference frequency ω_0. Condition $|\delta_s|\lesssim 1$ determines practically convenient choice of ω_0. $D_s=D(\delta_s)$ is the normalized wave number shift, $D_s'=\partial_\delta D(\delta_s)$ characterizes the group velocity shift, and $D_s''=\partial_\delta^2 D(\delta_s)<0$ is the GVD at the soliton frequency. Physical group velocity V at the frequency $\omega=\omega_0+\delta/\tau$ is given by

$$V(\delta) = \frac{v_0}{1+\{v_0\tau/L_{gvd}\}\partial_\delta D(\delta)}. \qquad (5)$$

The solution [Eq. (4)] is fully characterized by the parameters $q>0$ and δ_s, and is an exact solution of Eq. (1) providing that: (i) $\theta=0$ and (ii) all derivatives of the function $F(\xi)$ higher than second are disregarded.

To proceed further we fix $\theta=0$ and present solution of Eq. (1) in the form

$$A = [F(\xi)+g(z,\xi)]e^{iz[D_s+q]-i\delta_s t}, \quad \xi \equiv t - zD_s'. \qquad (6)$$

Assuming that g is small we disregard all the terms nonlinear in g and derive

$$i\vec{P} = \partial_z\vec{g} + i\hat{\mathcal{L}}\vec{g}, \quad \vec{g} = [g, g^*]^T. \qquad (7)$$

Here

$$\hat{\mathcal{L}} = \begin{bmatrix} \hat{W} & -F^2 \\ F^{*2} & -\hat{W}^* \end{bmatrix}, \qquad (8)$$

where

$$\hat{W} = q + \frac{1}{2}D_s''\partial_\xi^2 - 2|F|^2 - [D(i\partial_\xi+\delta_s) - D_2(i\partial_\xi)], \qquad (9)$$

and

$$\vec{P} = [p, -p^*]^T, \quad p = [D(i\partial_\xi+\delta_s) - D_2(i\partial_\xi)]F, \qquad (10)$$

$$D_2(i\partial_\xi) = D_s + iD_s'\partial_\xi - \frac{1}{2}D_s''\partial_\xi^2. \qquad (11)$$

$\vec{P}$ is localized in ξ and in order for Eq. (7) to have a localized solution it is enough that the null subspace of the operator adjoint to $\hat{\mathcal{L}}$ is orthogonal to $\vec{P}$. The dispersion operator is a polynomial and therefore it is possible to show that $D(i\partial_\xi+\delta_s)=D_2(i\partial_\xi)+\Sigma_{m=3}^{M} i^m/m!\,D_s^{[m]}\partial_\xi^m$. Coefficients $D_s^{[m]}/m!$ for $m\geqslant 3$, where $D_s^{[m]}=\partial_\delta^m D(\delta_s)$, should be considered as small parameters by virtue of the assumption that Eq. (4) is the solution in the main order of the perturbation theory. However, frequency of the perturbation g can be large. Therefore, third and higher order derivatives can counterbalance smallness of the dispersion coefficients. That is why the higher

order corrections to the dispersion are kept not only in $\vec{P}$, but also inside $\hat{\mathcal{L}}$. For all terms in $\hat{\mathcal{L}}$ to be balanced we require

$$|[D(i\partial_\xi + \delta_s) - D_2(i\partial_\xi)]g| \lesssim \frac{1}{2}|D_s''\partial_\xi^2 g|. \tag{12}$$

Practically Eq. (12) imposes upper boundary on the values of the frequency detuning between the soliton and the perturbation g correctly described by Eq. (7). For example, for $M=3$, see Eq. (2), and fixing the time dependence of g as $e^{i\xi[\delta_s-\delta]}$, we find that for Eq. (12) to work we have to require $|\epsilon[\delta-\delta_s]| \lesssim |D_s''/2| \sim O(1)$, where

$$\epsilon = \frac{\partial_\omega \beta_2(\omega_0)}{6\tau|\beta_2(\omega_0)|}. \tag{13}$$

Keeping only ∂_ξ^3 in $\hat{\mathcal{L}}$ already makes existence of the localized $\vec{g}$ impossible [16,19,20,22]. This is because ∂_ξ^3-term adds an extra zero eigenvalue to the continuous spectrum of $\hat{\mathcal{L}}^\dagger$ with the corresponding eigenfunction not being orthogonal to $\vec{P}$. The corresponding *resonant* frequency can be found if one seeks the eigenfunction of the continuum in the form $e^{i\lambda z + i[\delta_s-\delta]\xi}$, then the eigenvalues λ are given by

$$-\lambda = q + D_s - [\delta_s - \delta]D_s' - D(\delta). \tag{14}$$

Physically the resonance is achieved when the soliton and a dispersive wave have the same wave number, i.e., $\lambda=0$, and therefore

$$q + D_s - [\delta_s - \delta_r]D_s' = D(\delta_r). \tag{15}$$

Equation (15) is an equation for δ_r. Real δ_r's correspond to the resonant nonlocalized waves and δ_r/τ is the frequency detuning from ω_0. Geometrical meaning of Eq. (15) is clear. Its left-hand side is a tangent to the $D(\delta)$ curve taken at $\delta=\delta_s$ and shifted up by q. Remembering that D_s'' must be negative for the soliton to exist, one can show that the pairs of real δ_s and δ_r satisfying Eq. (15) can always be found providing that $\partial_\delta^2 D(\delta)$ changes its sign. All complex roots of the polynomial Eq. (15) correspond to the waves exponentially decaying for ξ tending to either $-\infty$ or $+\infty$ and describe localized corrections to the soliton (4) [21].

GVD changes its sign at least once in most optical fibers including PCFs. The PCF used in Ref. [7] changes GVD sign twice, similar to the fiber described in Ref. [25], and therefore has the finite spectral range with anomalous GVD, see Fig. 1(a). The corresponding dependencies of the real resonant frequencies δ_r from the soliton frequency δ_s are shown in Fig. 1(b). An important feature of Fig. 1(b) is that $|\delta_r - \delta_s|$ reaches its minimum values, when the soliton frequency approaches the zero GVD points.

For qualitative understanding of the resonances shown in Fig. 1(b) it is sufficient to consider cubic approximation for $D(\delta)$

$$D(\delta) = -\frac{\delta^2}{2} + \epsilon\delta^3, \tag{16}$$

where sgn $\beta_2(\omega_0)=-1$. Using the Cardano's formula, we get the expression for δ_r:

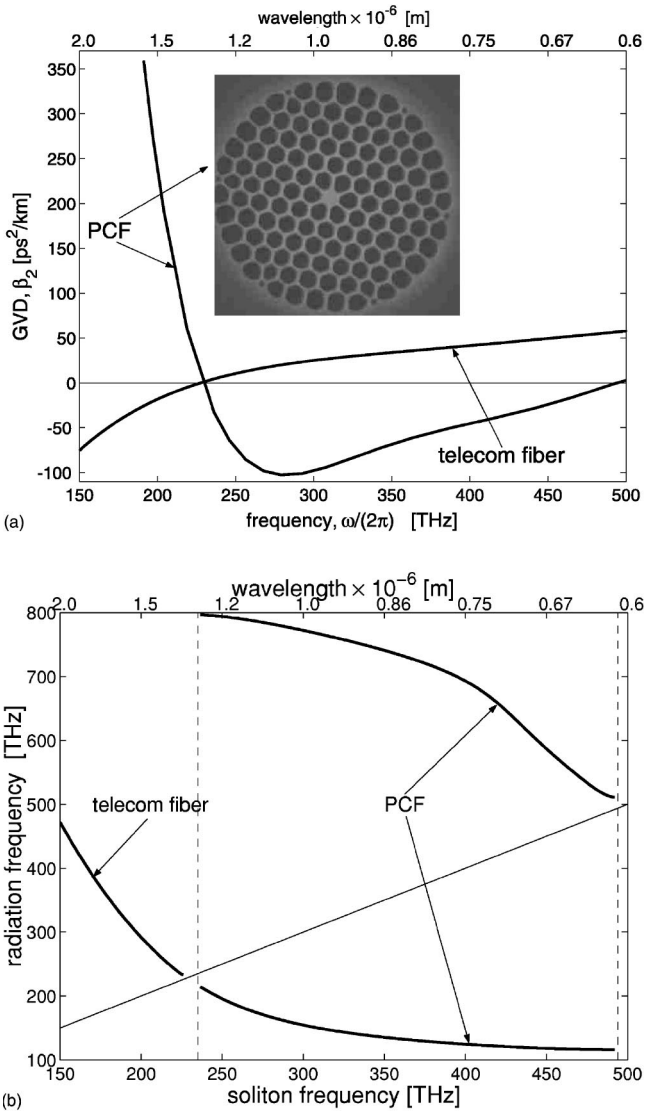

FIG. 1. (a) Electron micrographs of the PCF from Ref. [7] and corresponding $\beta_2(\omega)$ and $\beta_2(\omega)$ for the telecom fiber (SMF28) is also shown. The core diameter of the PCF shown is $\simeq 1.2$ μm, (b) dependencies of the resonance frequencies δ_r from the soliton frequency δ_s. Vertical dashed lines mark the zero GVD points in the PCF. The diagonal line marks the boundary where the radiation and soliton frequencies coincide. The radiation branches above/below the diagonal line are, respectively, blue/redshifted relative to the soliton carrier frequency. Radiation frequency in the telecom fiber is also shown.

$$\delta_r = \frac{1}{12\epsilon}[2 + 4(1 - 6\epsilon\delta_s)^2 Y^{-1/3} + Y^{1/3}], \tag{17}$$

where $Y = 8X + 6\epsilon\sqrt{6q[X - 54q\epsilon^2]}$, $X = 1 - 18\delta_s\epsilon + 108q\epsilon^2 + 108\delta_s^2\epsilon^2 - 216\delta_s^3\epsilon^3$. The only real value of δ_r is selected by choosing the appropriate branch of $Y^{1/3}$.

Assuming $\epsilon \ll 1$, $|\delta_r - \delta_s|\epsilon \sim O(1)$ one can calculate an approximate analytical expression for the resonant frequency [16,22]:

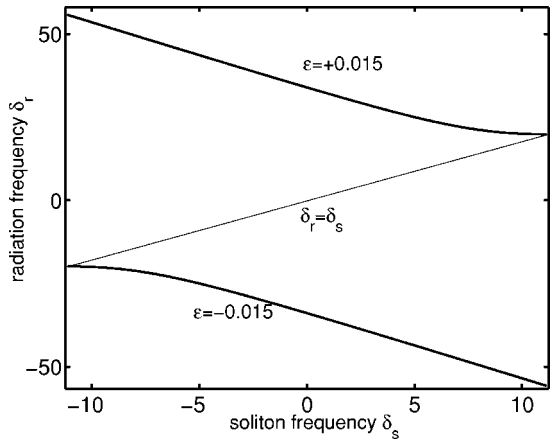

FIG. 2. Resonant frequency δ_r as function of the soliton frequency δ_s for the dispersion profile (16): $q=10$ and $\epsilon=\pm 0.015$. The diagonal line marks the boundary where the radiation and soliton frequencies coincide.

$$\delta_r - \delta_s = \frac{1}{2\epsilon} + O(1). \tag{18}$$

For example, at $\lambda=1.15$ μm, i.e., $\omega=2\pi\times 239$ THz, the fiber in Fig. 1(a) has $\beta_2=-47$ ps^2/km and $\beta_3=-0.5$ ps^3/km, which gives $\epsilon\simeq -0.015$ for $\tau=120$ fs. It is clear from Eq. (18) that the positive/negative slopes of $\beta_2(\omega)$ are responsible for the radiation bands, which are blue/redshifted from the soliton. Figure 2 shows graphs of δ_r vs δ_s as given by Eq. (17). The above consideration of the cubic dispersion also explains why the two radiation bands exist in the fibers with $\beta_2(\omega)$ having two zeros, see Fig. 1. Note, that the condition (12) is satisfied for (18).

B. Amplitude of the radiation field

Finding the amplitude of the emitted wave is a technically involved problem. Previous semiexplicit results by Wai *et al.* [16] and by Karpman [19,20] include undetermined constants, which can be computed only numerically. Our modeling indicates that the fully explicit analytical answers derived by Akhmediev and Karlson [22] and Karpman [21] do not match with the direct numerical solution of Eq. (1) for parameters relevant for the experiment [7]. The primary reason for this is that the theories in Refs. [21,22] do not account for the important F^2 terms inside $\hat{\mathcal{L}}$. Therefore, we develop our own approach, which further advances the methodology used in [19–22] and leads to the results, which agree well with direct modeling of Eq. (1).

It is clear that the radiation takes energy from the soliton and efficiency of this transfer increases as detuning of the radiation from the soliton carrier frequency decreases. If the radiation is far detuned from the spectral center of the soliton, then it should be weak and negligible. Therefore, considering the PCF example shown in Fig. 1 we can assume that the blueshifted radiation emitted by the soliton with the carrier frequency close to the left zero GVD point can be safely disregarded compared to the redshifted radiation, see Fig. 1(b). Thus, in this case and obviously in the case of the cubic dispersion (16) one can represent the radiation field in the form

$$g(z,\xi) = G(z,\xi)e^{-i\xi[\delta_r-\delta_s]}. \tag{19}$$

The assumption enabling us to advance the previously developed methods is that the amplitude G is a slow function of ξ compared to the oscillating exponential factor. After substitution of Eq. (19) into Eq. (7) we neglect all ξ-derivatives of G higher than first and find that G obeys

$$-i\partial_z G + i\{D_s' - D_r'\}\partial_\xi G - F^2\{2G + G^* e^{2i\xi[\delta_r-\delta_s]}\} = K(\xi), \tag{20}$$

where

$$K(\xi) \equiv e^{i\xi[\delta_r-\delta_s]}[D(i\partial_\xi + \delta_s) - D_2(i\partial_\xi)]F. \tag{21}$$

Contribution of the term containing G^* into the effective potential created by the soliton also can be disregarded providing that $q \ll |\delta_r-\delta_s||D_s'-D_r'| \sim \epsilon^{-2}$. By neglecting this term we are actually neglecting one of the two fundamental solutions to the left-hand side of Eq. (20). The inequality stated above ensures that the frequency of the driving term (21) is detuned far from the frequency of the neglected fundamental solution. Thus our final equation is

$$-i\partial_z G + i\{D_s' - D_r'\}\partial_\xi G - 2F^2 G = K(\xi). \tag{22}$$

One can easily see that the resonance frequency for this equation is zero, which reflects that we have accounted only for one real root of Eq. (15). Inclusion of all the higher order derivatives of G will recover the exact fiber dispersion together with all the disregarded complex and real resonances.

The exact solution of Eq. (22) obeying zero initial conditions at $z=0$ can be found in the integral form:

$$G(\xi,z) = \frac{e^{-iS(\xi)}}{i[D_s' - D_r']}\int_{\xi+[D_s'-D_r']z}^{\xi} d\xi' e^{iS(\xi')}K(\xi'), \tag{23}$$

where

$$S(\xi) = \frac{2\sqrt{-2qD_s''}}{[D_s' - D_r']}th\left(\frac{\xi}{w}\right). \tag{24}$$

The integral (23) cannot be taken in the explicit form. However the limit values of G can be found. Fixing $|\{D_s' - D_r'\}z/\xi| > 1$, one can show that for $D_s' - D_r' > 0$:

$$\lim_{z\to\infty,\xi\to-\infty} G = \frac{-e^{-iS(-\infty)}\mathcal{I}}{i[D_s' - D_r']}, \quad \lim_{z\to\infty,\xi\to\infty} G = 0, \tag{25}$$

and for $D_s' - D_r' < 0$

$$\lim_{z\to\infty,\xi\to-\infty} G = 0, \quad \lim_{z\to\infty,\xi\to\infty} G = \frac{e^{-iS(\infty)}\mathcal{I}}{i[D_s' - D_r']}, \tag{26}$$

where

$$S(\pm\infty) = \pm\frac{2\sqrt{-2qD_s''}}{D_s' - D_r'}, \tag{27}$$

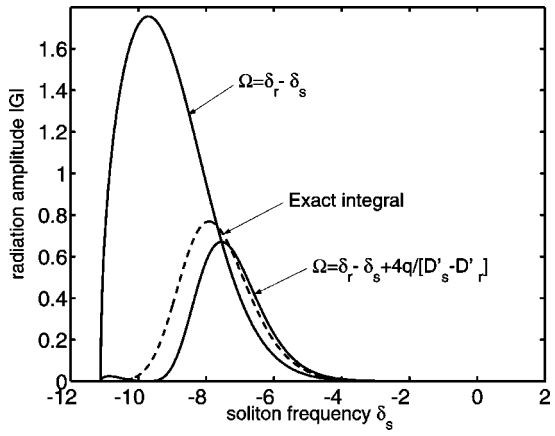

FIG. 3. Amplitude of the emitted wave $|G|$ calculated using Eqs. (25) and (28)—dashed line; using Eqs. (25) and (29) with Ω given by Eq. (30)—full line; using Eqs. (25) and (29), but with $\Omega=\delta_r-\delta_s$—full line, $\epsilon=-0.015$ and $q=3.5$.

$$\mathcal{I}=\int_{-\infty}^{\infty} d\xi e^{iS(\xi)}K(\xi). \tag{28}$$

The influence of the potential term on the amplitude is twofold. First, it affects the asymptotic value of the phase of the emitted wave. Second, and more important, it rotates the phase of the expression under the integral, which changes the amplitude of the emitted wave. Inside the area of localization of the integrand $K(\xi)$ the *th* function entering $S(\xi)$ can be replaced by its linear in ξ approximation, then $\mathcal{I}$ is simply the Fourier amplitude of the source term K calculated at the frequency Ω:

$$\mathcal{I}(\Omega)\simeq -\pi\sqrt{-D_s''}[D(\Omega+\delta_s)-D_2(\Omega)]\mathrm{sech}\left(\frac{\pi w}{2}\Omega\right), \tag{29}$$

where

$$\Omega=\delta_r-\delta_s+\frac{4q}{D_s'-D_r'}. \tag{30}$$

Taking the cubic dispersion Eq. (16) one can show that $D(\Omega+\delta_s)-D_2(\Omega)=\epsilon\Omega^3$ and $D_s'-D_r'=-1/[2\epsilon]+O(1)$. From the latter it follows that, when the detuning of the radiation from the soliton frequency is large enough the last term in Eq. (30) is much smaller than $|\delta_r-\delta_s|$. Thus, the importance of the potential term increases when the radiation and soliton frequencies become closer, see Figs. 1(b) and 2. It is crucial, however, that $\mathcal{I}$ has an exponential sensitivity in Ω. Therefore the higher order corrections to Ω which are small relative to $|\delta_r-\delta_s|$ can and indeed result far from negligible changes of $\mathcal{I}$. Therefore only absolutely small, i.e., $\ll 1$, corrections to Ω can be disregarded. Parameters close to the experimental conditions of Ref. [7] and to the numerical modeling carried out below give $|\delta_r-\delta_s|\sim 10$ and $4q/[D_s'-D_r']\sim 1$. The next order correction to Ω is expected to be $\ll 1$ and therefore it should indeed have small effect on the radiation amplitude. Obviously the rigorous proof of this can be obtained only calculating the next order correction to the radiation field, but this goes beyond our present scope and we simply rely on a good agreement of our analytical and numerical results, see Fig. 3 and Sec. IV. In Fig. 3 we show the dependence of the amplitude of the emitted wave versus δ_s calculated using Eqs. (25) and (28), using the approximation (29) and (30) and using (29), but with $\Omega=\delta_r-\delta_s$, i.e., disregarding contribution from the potential. One can see that as δ_r approaches δ_s the discrepancy between the formulas taking or disregarding the F^2-potential increases. For example, for $\delta_s=-6$, which is the value taken from the numerical results shown in Figs. 4(a) and 6(a), use of Eq. (30) gives $|G|\simeq 0.25$ and use of $\Omega=\delta_r-\delta_s$ gives $|G|\simeq 0.12$. This implies that our results and results of [21,22] differ by the factor $\simeq 2$ for this particular choice of parameters.

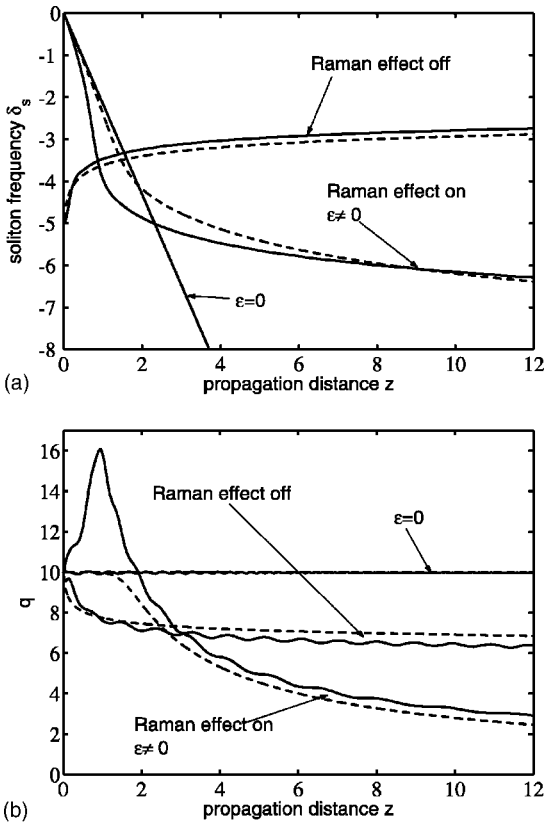

FIG. 4. (a) Soliton frequency δ_s as function of z, (b) soliton parameter q as function of z. Numerical modeling of Eq. (1) is shown by the full lines and of Eqs. (34) and (35) by the dashed lines: $\epsilon=-0.015$.

Note here that if one solves Eq. (1) initialized with a soliton having some chosen values of q and δ_s, then it becomes clear that parameters of the soliton and parameters of the radiation are changing with propagation. Therefore in order for the analytics to be properly compared with numerics we should generalize the former by allowing adiabatic z dependence of the soliton parameters.

IV. COMPENSATION OF THE SOLITON SELF-FREQUENCY SHIFT

It has been demonstrated previously [19,22] that solitons emitting resonant radiation lose energy slowly (i.e., nonex-

ponentially) transferring it to the resonant dispersive wave. To conserve the momentum integral the carrier frequency of the radiating soliton gets shifted in the spectral direction opposite to that of the radiation. This is the so-called spectral recoil effect [22]. This process, however, is expected to be frustrated by the soliton self-frequency shift towards the red part of the spectrum due to the Raman effect. The Raman shift is known to be a strong effect for pico- and femtosecond pulses [24].

The amplitude of the resonant wave has exponential dependence on $|\delta_r - \delta_s|$, see sech function in Eq. (29). The red Raman shift of the soliton carrier frequency, is directly proportional to the propagation distance z [23,24], therefore for fibers with the negative slope of $\beta_2(\omega)$, the Raman effect automatically reduces $|\delta_r - \delta_s|$, see Figs. 1(b) and 2, and leads to the exponential in z increase of the radiation amplitude with the rate $\simeq \pi|\partial_z[w\Omega]|/2$. The growing red radiation, however, presses the soliton towards the blue side of the spectrum. Thus, there exists the possibility of a balance between the red frequency shift due to the Raman effect and the blueshift coming from the radiation pressure. This effect has been suggested and considered as the prime reason for the existence of the solitary pulses with the compensated Raman self-frequency shift and the growing tail of the resonant radiation observed in Ref. [7]. The theory of this effect based on the results of Secs. II and III is developed below.

A. Adiabatic theory

The essence of our approach is the standard assumption that the soliton parameters δ_s and q vary slowly in z. Then using evolution equations for the momentum and power integrals we derive a system of ordinary differential equations governing dynamics of δ_s and q.

The momentum integral

$$M = \int dt|A|^2 \partial_t \arg A = \frac{1}{2i}\int dt[A^* \partial_t A - A\partial_t A^*] \quad (31)$$

has physical meaning of the average frequency and is a conserved quantity of Eq. (1), i.e., $\partial_z M = 0$, only if Raman effect is disregarded. Using Eq. (1) one can show that

$$\partial_z M = -\int dt\left\{\partial_t|A|^2 \int dt'[R(t-t') - \Delta(t-t')]|A(t')|^2 dt'\right\}. \quad (32)$$

The power integral

$$Q = \int dt|A|^2 \quad (33)$$

is a conserved quantity even in the presence of the Raman effect. We now assume that the radiation tail is long enough so that contributions to M and Q originating from the overlap between the radiation and soliton are negligible compared to the momenta and power of the radiation and soliton taken separately. Then M and Q can be approximated by $M \simeq M_s + M_r$ and $Q \simeq Q_r + Q_s$, where $M_{s,r}$ and $Q_{s,r}$ are momenta and powers of the soliton and radiation parts of the field, respectively.

Using Eqs. (6), (25), and (28) and the conservation law $\partial_z Q = 0$ we find in the leading approximation the equation governing evolution of the soliton parameter q:

$$\partial_z q = -\frac{|\mathcal{I}|^2}{\partial_q Q_s |D_s' - D_r'|}. \quad (34)$$

Similarly, substituting Eqs. (6), (25), and (28) into Eq. (32) we find the equation for the soliton frequency:

$$Q_s \partial_z \delta_s = [\delta_s - \delta_r]\partial_z Q_r - \alpha. \quad (35)$$

Here $\alpha \equiv 4\tau_r(2q)^{5/2}/[15|D_s''|^{1/2}]$, $\tau_r \simeq 3fs/\tau$ characterizes the slope of the Raman gain spectrum [24], $Q_s = \int d\xi |F|^2 = 2\sqrt{2q|D_s''|}$, $Q_r = z|\mathcal{I}|^2/|D_s' - D_r'|$, and $\partial_z Q_r \simeq |\mathcal{I}|^2/|D_s' - D_r'|$.

By neglecting the first term on the right-hand side of Eq. (35) one reproduces the standard formula for the Raman induced soliton self-frequency shift [23,24], while the $\partial_z Q_r$ term describes evolution of the soliton frequency due to radiation pressure. Taking separately, the influence of the radiation and the Raman effect on the soliton frequency have been reported in Refs. [22,23], respectively. The possibility for them to balance each other has been recently demonstrated experimentally and numerically in [7]. Equation (35) provides analytical interpretation of the results of Ref. [7]. Indeed, for $\delta_s - \delta_r > 0$, i.e., for the redshifted radiation, the terms on the right-hand side can counterbalance one another. The balance clearly critically depends on the soliton frequency. However, one cannot expect exact frequency locking, i.e., $\partial_z \delta_s = 0$, for δ_s satisfying $\alpha = [\delta_s - \delta_r]|\mathcal{I}|^2/|D_s' - D_r'|$. This is because q is not constant, see Eq. (34), but decays with z due to leakage of the radiation out of the soliton.

B. Numerical results

Throughout this subsection we present results of the direct numerical modeling of Eq. (1) and Eqs. (34) and (35) with dispersion (16) and $\epsilon = -0.015$. Approximation of the cubic dispersion is sufficient for the qualitative explanation of the experimental observations of Ref. [7] and in addition it significantly simplifies handling of the right-hand sides of Eqs. (34) and (35). The latter is because for the cubic dispersion we know the exact analytical dependence of δ_r on q and δ_s, see Eq. (17).

Figure 4 shows evolution of the soliton parameters δ_s and q calculated directly from Eq. (1) and from the coupled system of the adiabatic Eqs. (34) and (35). We show three different cases. The first case is with the Raman effect switched off and $\epsilon = -0.015$. Then the radiation action on the soliton naturally leads to the decay of the soliton amplitude and to the blueshift of its frequency. The second case with the Raman effect on and $\epsilon = 0$, i.e., there is no resonant radiation. In this case q is practically constant and the standard redshift of the soliton frequency is observed. The third and last case is when both Raman and radiation effects are switched on. One can see that in this case the soliton amplitude drops faster than with the Raman effect off, and that the rate of change of the soliton frequency is much less than the Raman only rate. The faster decrease of q happens because for small z more and more photons are transferred to the radiation because

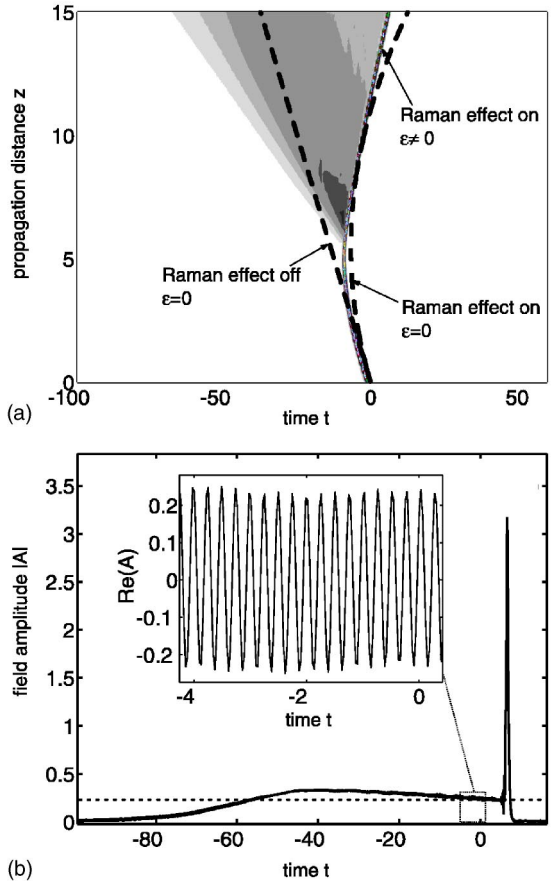

FIG. 5. (a) Spatiotemporal evolution of $|A|$ as obtained from numerical modeling of Eqs. (1) and (16) with initial condition given by Eq. (4) and $\delta_s(z=0)=5$, $q(z=0)=10$, $\epsilon=-0.015$. Gray shaded region emerging from the soliton is the radiation field. The gray scale map used exaggerates the strength of the radiation in order to show it clearly. Dashed lines mark the soliton trajectories with radiation and/or Raman effects switched off, (b) $|A|$ as a function of t extracted from (a) at $z=15$. Dotted horizontal line indicates the analytical result for the radiation amplitude calculated from Eqs. (26) and (28). The inset in (b) shows the fine details of Re A vs t.

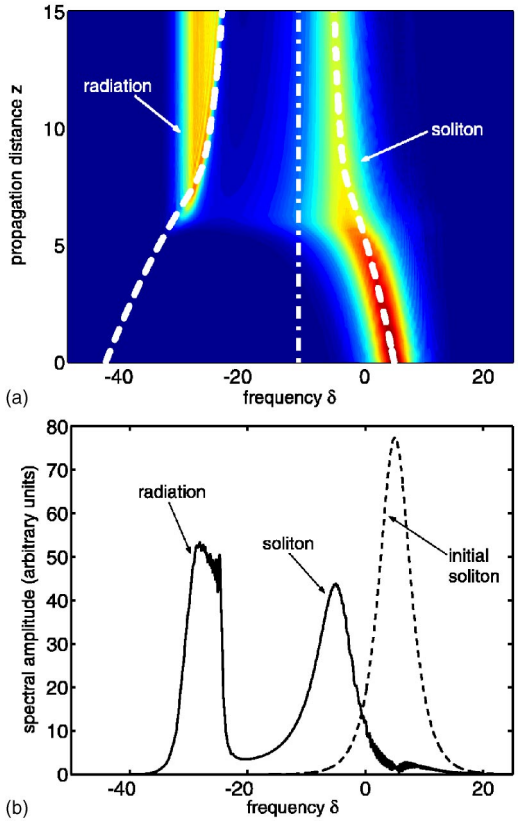

FIG. 6. (Color online) (a) z evolution of the amplitude of the Fourier transform of A as obtained from numerical modeling of Eqs. (1) and (16). Dashed lines are the results of the adiabatic theory. Dashed-dotted line marks the zero GVD point, (b) image of the amplitude of the Fourier transform of A for $z=15$; all parameters as for Fig. 5.

$|\delta_r-\delta_s|$ is continuously reduced by the Raman effect. As amplitude of the radiation increases so is the recoil on the soliton, therefore the rates of change of q and δ_s decrease substantially for larger values of z. With GVD having the opposite slope, i.e., for $\epsilon>0$, the recoil effect pushes the soliton towards the red side of the spectrum and therefore acts in the same spectral direction as the Raman effect. The overall effect is that $|\delta_r-\delta_s|$ is continuously increased and therefore the radiation amplitude decreases with z.

Figures 5(a) and 5(b) show the soliton evolution in the (t,z)-plane and image of the absolute value of the field amplitude for a given z. Figures 6(a) and 6(b) show the soliton evolution in the (δ,z) plane and image of the absolute value of the spectral amplitude of the field. For $\epsilon=0$ and the Raman effect switched off the soliton trajectory in the (t,z)-plane is a straight line, i.e., $t/z=$const, with slope determined by the initial value of δ_s. The slope is preserved with z due to Galilean invariance of the ideal NLS equation [20]. With the Raman effect on the soliton trajectory becomes parabolic, i.e., $t/z^2=$const, which corresponds to the soliton group velocity being inversely proportional to z [23,24]. When the tail of the exponentially amplified radiation appears in the case with $\epsilon<0$ and the Raman effect on, the soliton trajectory becomes straight again, which indicates that the radiation and the Raman effect balance each other. Emergence of the strong radiation band, see Fig. 6(a), is accompanied by the transition from the regime of the uncompensated Raman induced self-frequency shift to the regime where the latter is substantially depleted. As one can see, the results of the adiabatic theory predict evolution of the blue edge of the radiation band, see Fig. 6(a). This indicates that parameters of the soliton taken for a given z determine parameters of the radiation emitted at the same z. Frequencies on the red edge and in the center of the radiation band have been created by the soliton at the previous values of z, when the soliton frequency was larger.

Radiation tail appearing on the left from the soliton in the (t,z)-plane implies that the red radiation propagates faster than the soliton, i.e., that it is emitted forward. This happens because $D_r'<D_s'$ and $V(\delta_r)>V(\delta_s)$, see Eq. (5). The Raman effect creates the negative acceleration and therefore causes delay of the solitons. The redshifted radiation, however, creates positive acceleration and therefore tends to bend the soliton trajectory in the opposite direction, which results in

the overall straightening of the trajectory. Oppositely, for the positive GVD slope the radiation is blueshifted. It is emitted backwards, $V(\delta_r) < V(\delta_s)$, and causes negative acceleration to the soliton.

Excellent qualitative and good quantitative agreement of the results of the adiabatic theory and of the direct numerical modeling of Eq. (1) confirms validity of our analytical results for the radiation amplitude derived in Sec. III. Comparison of the results presented here for the model dispersion (16) and results of Ref. [7] for the real PCF dispersion show that using of Eq. (16) captures the essential features needed to explain the effect of the self-frequency shift compensation reported in Ref. [7]. Overall, analytical and numerical results reported above confirm that the effect reported in Ref. [7] takes place indeed due to balance between the Raman induced soliton self-frequency shift and radiation pressure on the soliton.

V. DISCUSSION

In Ref. [7] where the effect of the self-frequency shift compensation by the radiation pressure has been originally reported uses the term "cancellation" instead of "compensation." However, as shown above analytically the exact cancellation is prevented because the soliton parameter q decreases with the propagation distance. In practical terms, however, the compensation is very strong indeed. For example, results shown in Figs. 4 and 6 being recalculated into the physical units show that over the propagation distance $\simeq 2$ m the uncompensated Raman shift of a $\simeq 120$ fs soliton is $\simeq 100$ THz. However, in the regime when the frequency of the soliton is quasilocked by the radiation, the frequency shift over the same distance is only $\simeq 5$ THz. This agrees well with experimental observations of Ref. [7].

For the long propagation distances the soliton keeps losing its energy to radiation and gets broader, therefore both recoil and Raman effects are weakening, but balance between the two preserves. For example for parameters of Fig. 5 the soliton decay rates found from the direct numerical modeling of Eq. (1) and measured in the inverse propagation units are 0.5, 0.15, 0.04, and 0.02 for the propagation distances 6, 12, 25, and 50, respectively. The corresponding values of the decrease rate of the soliton frequency are 0.15, 0.06, 0.025, and 0.01. In our modeling we observed propagation of the soliton over more than 100 dispersion lengths, but its final fate cannot be unambiguously determined from our results, because radiation finally passes through or gets reflected from the boundaries and feeds back into the soliton itself.

Previously reported methods to compensate the Raman induced soliton self-frequency shift in telecom fibers have involved different techniques for achieving the frequency dependent amplification or loss in the fibers [27–30] or involved cross-phase modulation effect [31,32]. None of these techniques have relied on the effect of the resonant radiation. For studies of the uncompensated soliton self-frequency shift and Raman amplification in PCFs with the positive GVD slope, see, e.g., Refs. [33,34].

The most important feature of the resonant radiation emitted by the soliton under the conditions considered above is that it is exponentially amplified due to the combined action of the Raman effect and the negative GVD slope. The idea is to use this effect for the parametric amplification with the signal frequency controlled by the GVD slope. Note, that generation of the resonant wave by the soliton is very different from the standard four-wave mixing and does not exhibit the usual symmetry between the Stokes and anti-Stokes waves. This is because in the process of the emission of the resonant wave by the soliton the energy and momentum are shared between the emerging wave on one side and the solitonic pulse as a whole on the other, but not between several continuous waves as in the usual four-wave mixing.

Localized solutions closely related to the solitons emitting resonant radiation are the solitons nesting on the top of the resonant wave extending from $-\infty$ to $+\infty$. These solitons are often called quasisolitons, see, e.g., Refs. [35–37]. If, for some selected parameters, the background amplitude becomes zero, then the quasisolitons are called embedded solitons [37–41]. Mathematical artificiality of the quasisolitons exhibits itself through the fact that they carry infinite energy, but their relevance to the physical reality can be inferred from the results presented above. Indeed disregarding the z derivative in Eq. (22) one can find its general solution in the form $G = G_i(\xi) + BG_h(\xi)$, where B is an arbitrary constant, $G_i = \exp[-iS(\xi)] \int_{-\infty}^{\xi} d\xi' \exp[-iS(\xi')] K(\xi')$ and $G_h = \exp[-iS(\xi)]$. Using boundary conditions $G(+\infty) = G(-\infty) e^{i2\phi}$, where ϕ is a constant phase shift, valid for the solitons on the infinite background, one can find B and the amplitude of the background at infinity: $|G(\pm\infty)| = b\mathcal{I}/|D_s' - D_r'|$, where $b = \{2|\sin[S(+\infty) + \phi]|\}^{-1}$. Thus, the amplitude of the infinite background of the quasisolitons differs from the amplitude of the semi-infinite background, emerging from the natural condition that initially there is no radiation, by the factor b, cf. Eq. (25). Other differences between the two types of quasisolitons have also been recently discussed in Ref. [42].

VI. SUMMARY

We have developed a comprehensive theory of the effect of the soliton self-frequency shift compensation by the radiation pressure in fibers with the negative slope of $\beta_2(\omega)$. Our results provide analytical underpinning for the recent experimental observations [7]. Our approach to calculation of the amplitude of the resonant radiation generalizes the previously known techniques by accounting for the potential created by the soliton, see Eqs. (23) and (25)–(29), which is essential for achieving good matching between the analytical and numerical results.

ACKNOWLEDGMENTS

The authors acknowledge J.C. Knight, F. Luan, P.St.J. Russell, and A.G. Vladimirov for stimulating discussions. We are grateful to F. Luan and N. Joly for the image of their fiber in Fig. 1(a). This work is partially supported by the EPSRC Grant No. GR/S20178/01.

[1] P. St. J. Russell, Science **299**, 358 (2003).
[2] B. J. Eggleton, C. Kerbage, P. Westbrook, R. S. Windeler, and A. Hale, Opt. Express **9**, 698 (2001).
[3] J. C. Knight, Nature (London) **424**, 847 (2003).
[4] T. M. Monro and D. J. Richardson, C. R. Phys. **4**, 175 (2003).
[5] L. F. Mollenauer, Science **302**, 996 (2003).
[6] W. H. Reeves, D. V. Skryabin, F. Biancalana, J. C. Knight, P. St. J. Russell, F. G. Omenetto, A. Efimov, and A. J. Taylor, Nature (London) **424**, 511 (2003).
[7] D. V. Skryabin, F. Luan, J. C. Knight, and P. St .J. Russell, Science **301**, 1705 (2003).
[8] F. Benabid, J. C. Knight, G. Antonopoulos, and P. St. J. Russell, Science **298**, 399 (2002).
[9] C. M. Smith, N. Venkataraman, M. T. Gallagher, D. Muller, J. A. West, N. F. Borrelli, D. C. Allan, and K. W. Koch, Nature (London) **424**, 657 (2003).
[10] D. G. Ouzounov, F. R. Ahmad, D. Müller, N. Venkataraman, M. T. Gallagher, M. G. Thomas, J. Silcox, K. W. Koch, and A. L. Gaeta, Science **301**, 1702 (2003).
[11] J. K. Ranka, R. S. Windeler, and A. J. Stentz, Opt. Lett. **25**, 25 (2000).
[12] J. Herrmann, U. Griebner, N. Zhavoronkov, A. Husakou, D. Nickel, J. C. Knight, W. J. Wadsworth, P. St. J. Russell, and G. Korn, Phys. Rev. Lett. **88**, 173901 (2002).
[13] J. M. Dudley, L. Provino, N. Grossard, H. Maillotte, R. S. Windeler, B. J. Eggleton, and S. Coen, J. Opt. Soc. Am. B **19**, 765 (2002).
[14] J. H. V. Price, W. Belardi, T. M. Monro, A. Malinowski, A. Piper, and D. J. Richardson, Opt. Express **10**, 382 (2002).
[15] V. E. Zakharov, P. Guyenne, A. N. Pushkarev, and F. Dias, Physica D **152**, 573 (2001).
[16] P. K. A. Wai, H. H. Chen, and Y. C. Lee, Phys. Rev. A **41**, 426 (1990).
[17] P. K. A. Wai, C. R. Menyuk, H. H. Chen, and Y. C. Lee, Opt. Lett. **12**, 628 (1987).
[18] A. Höök and M. Karlsson, Opt. Lett. **18**, 1388 (1993); IEEE J. Quantum Electron. **30**, 1831 (1994).
[19] V. I. Karpman, Phys. Rev. E **47**, 2073 (1993).
[20] V. I. Karpman, Phys. Rev. E **62**, 5678 (2000).
[21] V. I. Karpman, Phys. Scr., T **82**, 44 (1999).
[22] N. Akhmediev and M. Karlsson, Phys. Rev. A **51**, 2602 (1995).
[23] J. P. Gordon, Opt. Lett. **11**, 662 (1986).
[24] G. P. Agrawal, *Nonlinear Fiber Optics* (Academic, San Diego, 2001).
[25] P. V. Mamyshev, P. G. J. Wigley, J. Wilson, G. I. Stegeman, V. A. Semenov, E. M. Dianov, and S. I. Miroshnichenko, Phys. Rev. Lett. **71**, 73 (1993).
[26] K. J. Blow and D. Wood, IEEE J. Quantum Electron. **25**, 2665 (1989).
[27] K. J. Blow, N. J. Doran, and D. Wood, J. Opt. Soc. Am. B **5**, 1301 (1988).
[28] D. Shenoy and A. Puri, Opt. Commun. **113**, 401 (1995).
[29] S. L. Liu and W. Z. Wang, Opt. Lett. **18**, 1911 (1993).
[30] A. S. Gouveia-Neto, A. S. L. Gomes, and J. R. Taylor, Opt. Lett. **14**, 514 (1989).
[31] C. S. Aparna, S. Kumar, and A. Selvarajan, Opt. Commun. **131**, 267 (1996).
[32] D. Schadt and B. Jaskorzynska, J. Opt. Soc. Am. B **5**, 2374 (1988).
[33] X. Liu, C. Xu, W. H. Knox, J. K. Chandalia, B. J. Eggleton, S. G. Kosinski, and R. S. Windeler, Opt. Lett. **26**, 358 (2001).
[34] Z. Yusoff, J. H. Lee, W. Belardi, T. M. Monro, P. C. Teh, and D. J. Richardson, Opt. Lett. **27**, 424 (2002).
[35] A. V. Buryak, Phys. Rev. E **52**, 1156 (1995).
[36] V. I. Karpman, A. G. Shagalov, and J. J. Rasmussen, Phys. Lett. A **293**, 247 (2002).
[37] V. E. Zakharov and E. A. Kuznetsov, J. Exp. Theor. Phys. **86**, 1035 (1998).
[38] M. J. Potasek and M. Tabor, Phys. Lett. A **154**, 449 (1991).
[39] E. M. Gromov and V. I. Talanov, Chaos **10**, 551 (2000).
[40] J. K. Yang, Phys. Rev. Lett. **91**, 143903 (2003).
[41] A. R. Champneys, B. A. Malomed, J. Yang, and D. J. Kaup, Physica D **152**, 340 (2001).
[42] V. I. Karpman, J. J. Rasmussen, and A. G. Shagalov, Phys. Rev. E **64**, 026614 (2001).